PNAS

Supporting Information for

Steering lithium and potassium storage mechanism in covalent organic frameworks by incorporating transition metal single atoms

Yingnan Cao[1], Qing Xu[2], Yi Sun[1], Jixin Shi[3], Yi Xu[1], Yongfu Tang[4], Xiudong Chen[5], Shuai Yang[6,7], Zheng Jiang[8], Han-Don Um[9], and Xiaopeng Li[3]*, Yong Wang[1]*

*Email of corresponding authors: xiaopeng.li@dhu.edu.cn (Xiaopeng Li); yongwang@shu.edu.cn (Yong Wang)

This file includes:
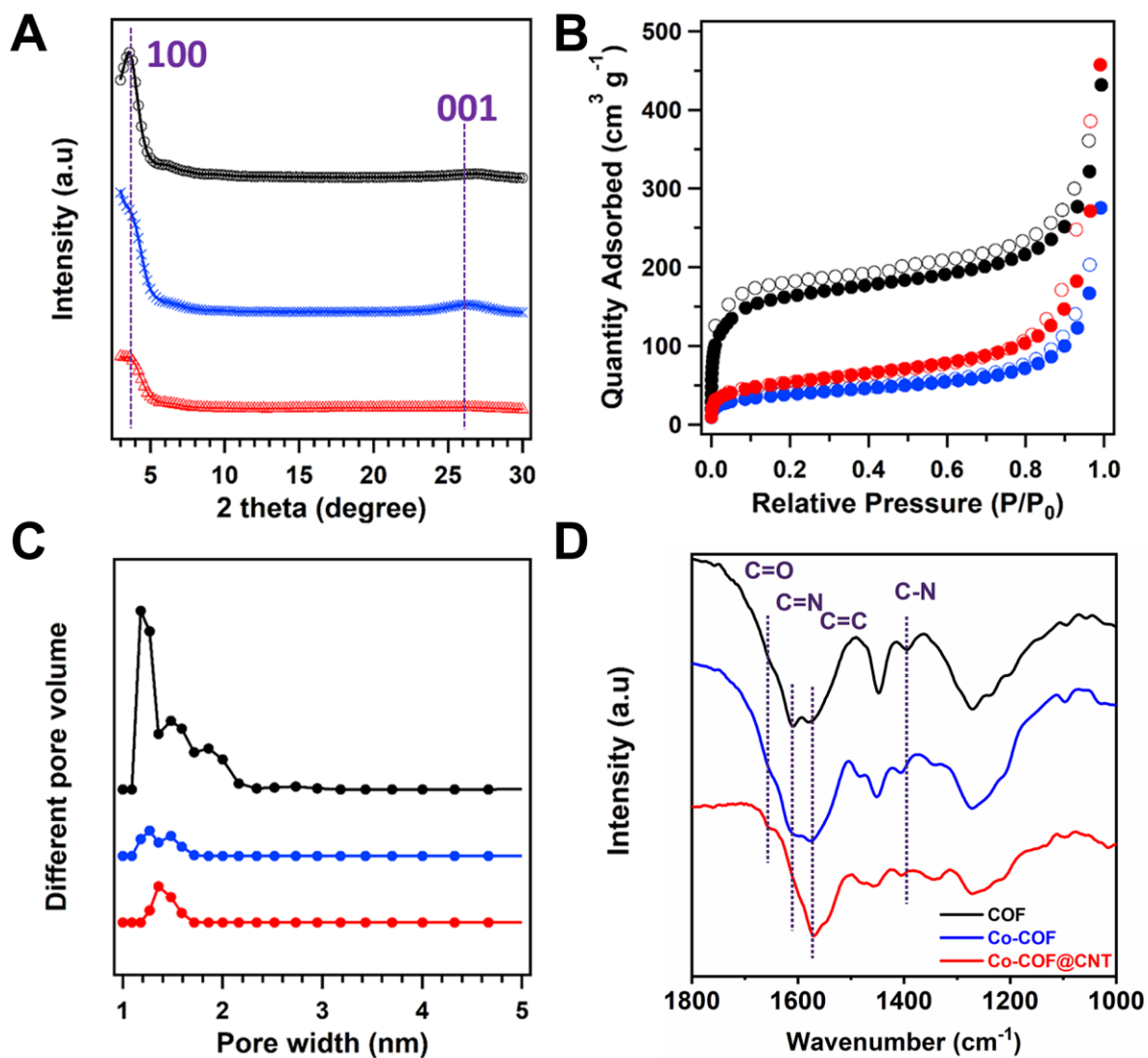
Supporting text
Figures S1 to S26
Tables S1 to S3

Fig. S1. Structure characterizations of TP-BPY-COF, Co-COF, and Co-COF@CNT. (**A**) PXRD patterns, (**B**) Nitrogen sorption isotherm profiles, (**C**) pore size distribution curves, and (**D**) FT-IR spectra. **Notes:** black, blue, and red stands for TP-BPY-COF, Co-COF, and Co-COF@CNT, respectively.
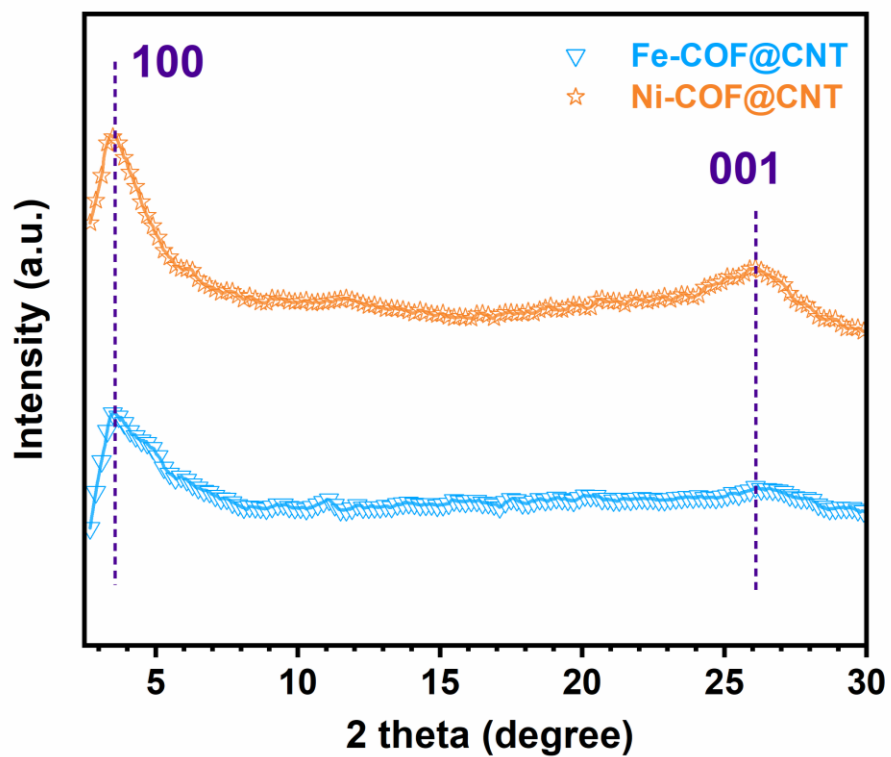
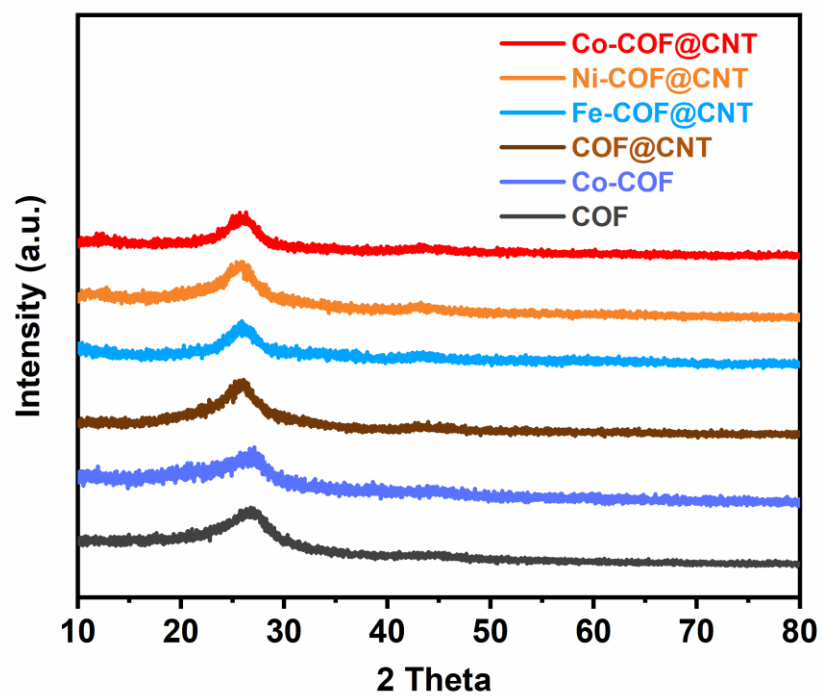**Fig. S2.** PXRD spectra of Fe-COF@CNT (blue) and Ni-COF@CNT (yellow).

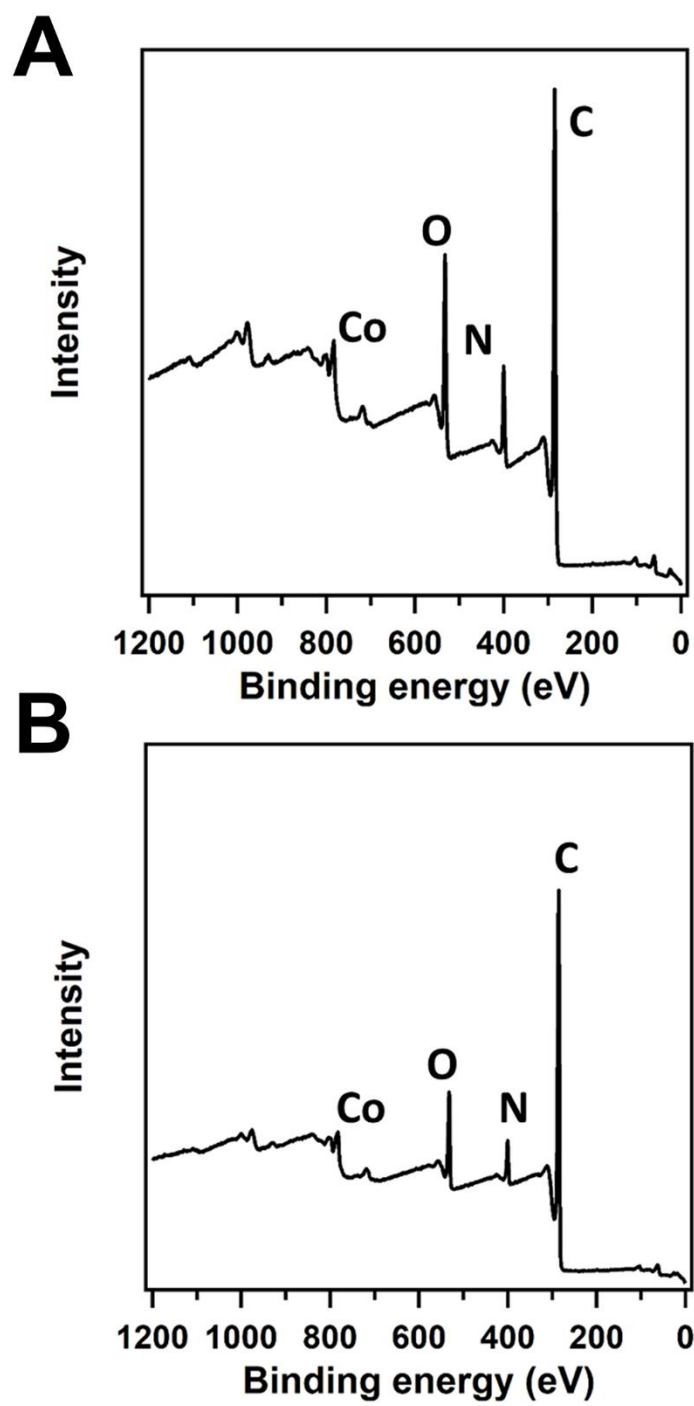**Fig. S3. PXRD spectra of various samples.**

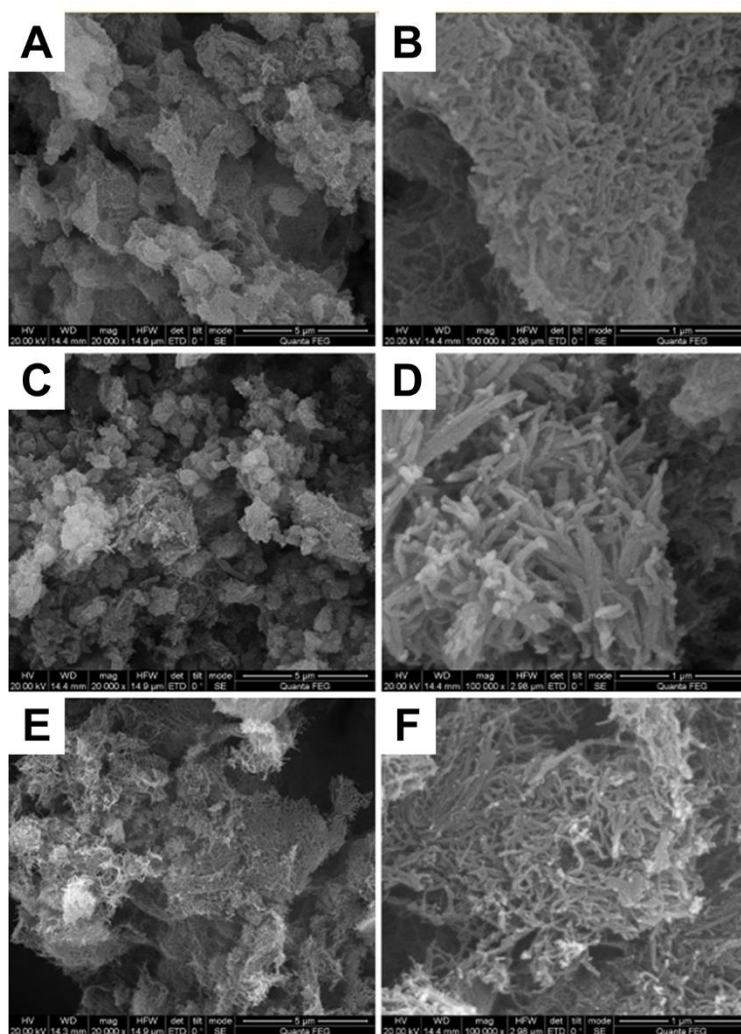**Fig. S4. The survey XPS spectrum of (A) Co-COF and (B) Co-COF@CNT.**

Fig. S5. SEM images of (A, B) TP-BPY-COF, (C, D) Co-COF, and (E, F) Co-COF@CNT.
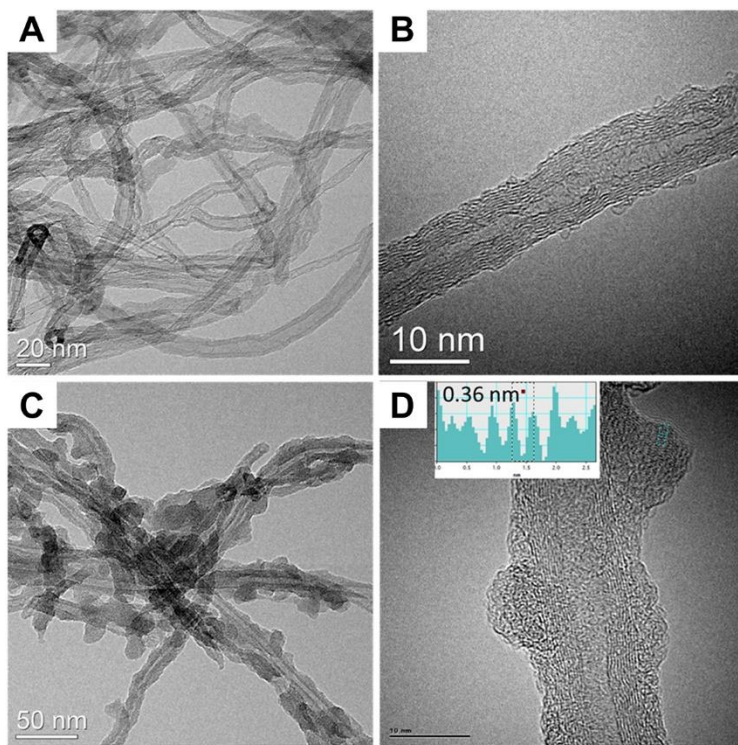
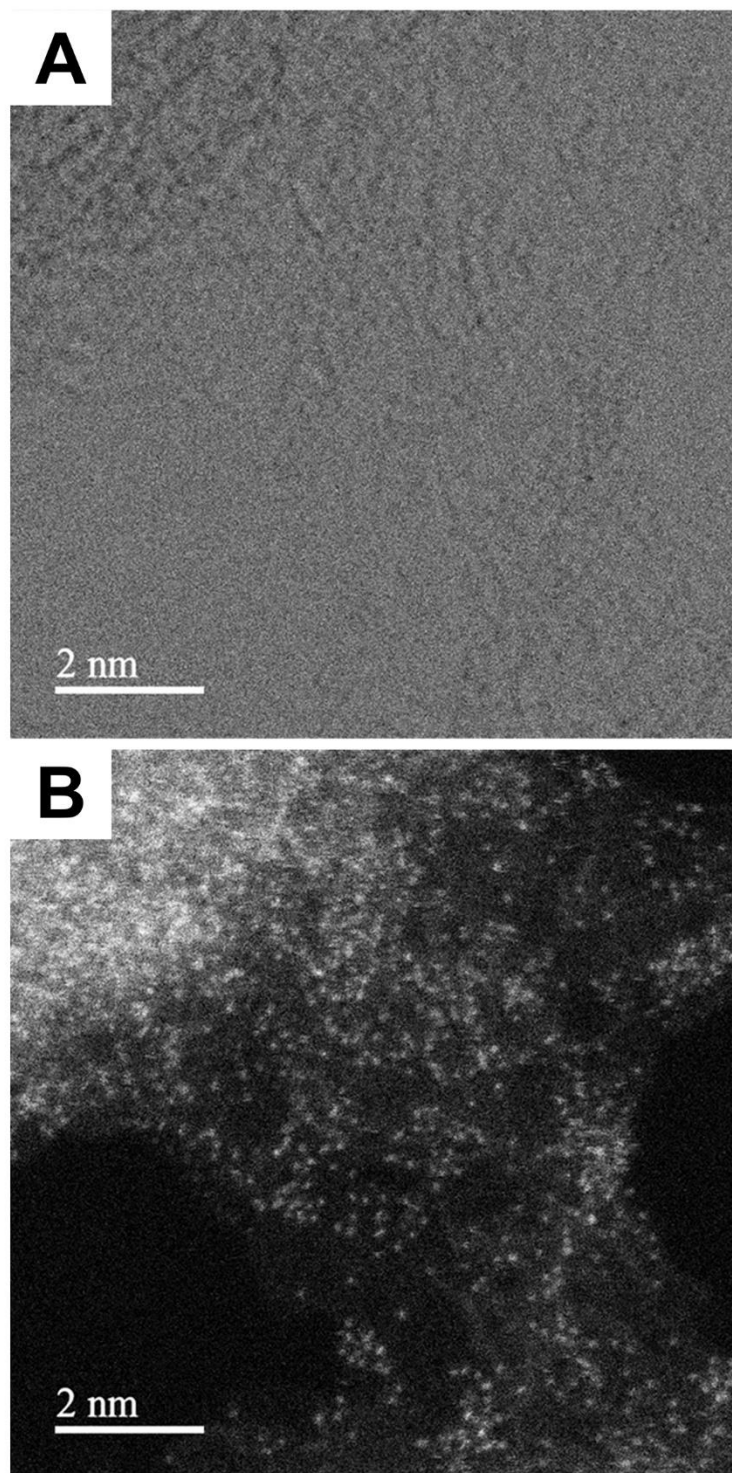**Fig. S6. TEM images of (A, B) CNT and (C, D) Co-COF@CNT.**

Fig. S7. (A) High-resolution bright-field TEM and (B) the corresponding HAADF-STEM images of Co-COF.
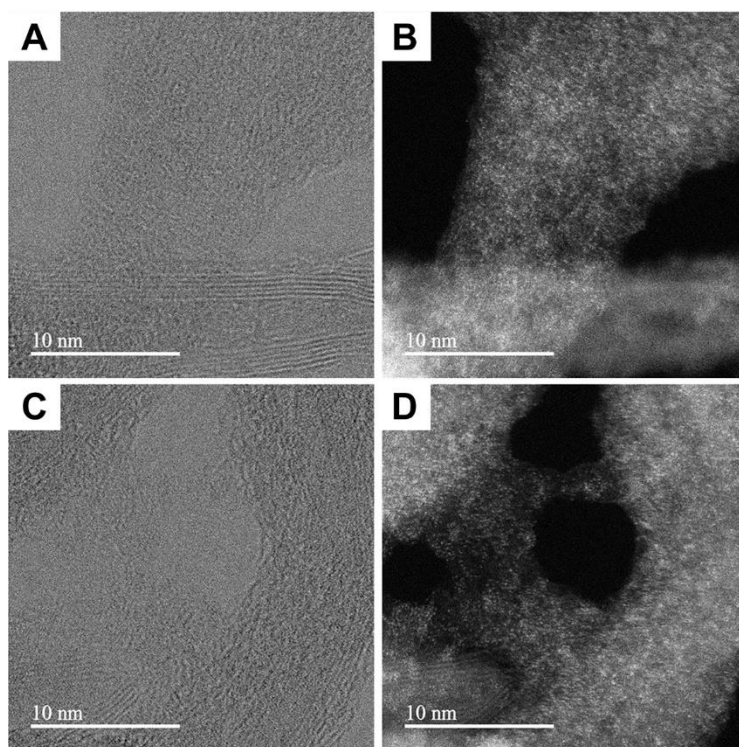
Fig. S8. (A, C) High-resolution bright-field TEM and (B, D) the corresponding HAADF-STEM images of Co-COF@CNT.
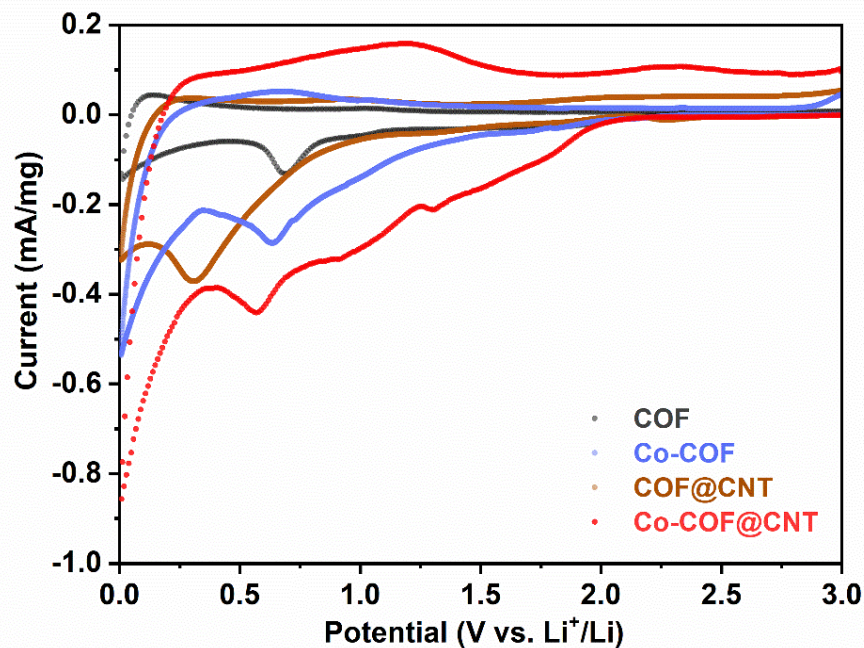
Fig. S9. Initial CV curves of the TP-BPY-COF, Co-COF, COF@CNT, and Co-COF@CNT electrodes for LIBs during 0.01-3.0 V at 0.1 mV s^{-1}. Notes: TP-BPY-COF (black), Co-COF (purple), COF@CNT (brown), and Co-COF@CNT (red).
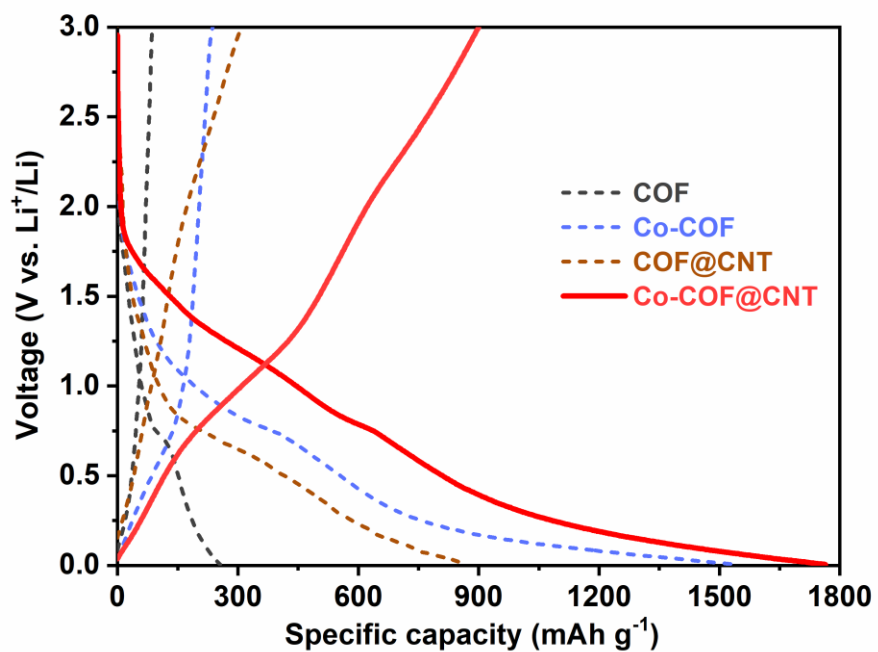
Fig. S10. Initial discharge and charge profiles of the TP-BPY-COF, Co-COF, COF@CNT, and Co-COF@CNT electrodes for LIBs at 100 mA g⁻¹. Notes: TP-BPY-COF (black), Co-COF (purple), COF@CNT (brown), and Co-COF@CNT (red).
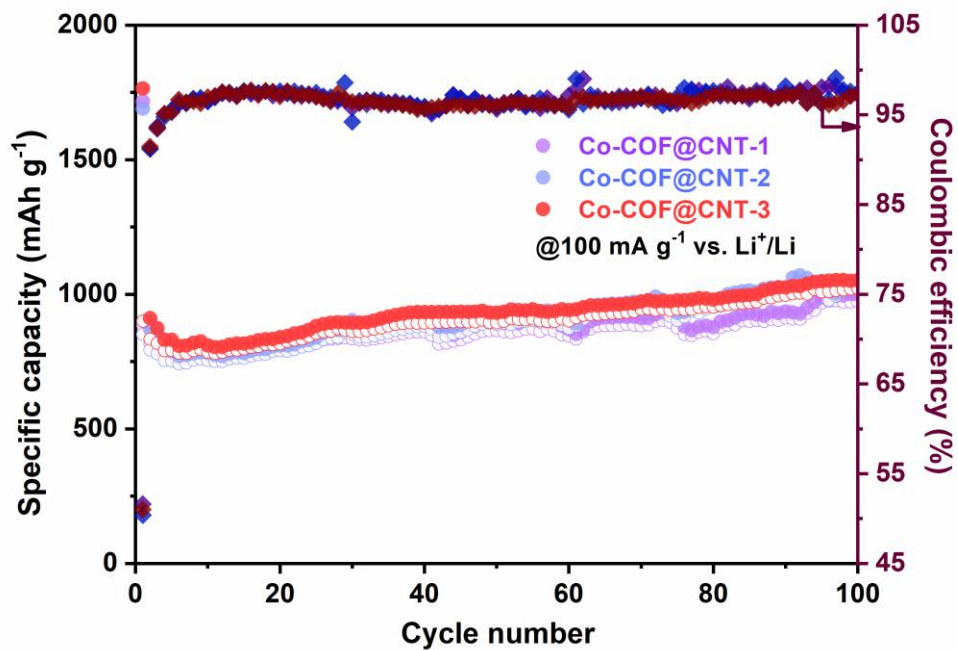
Fig. S11. Specific capacities and Coulombic efficiencies of the Co-COF@CNT electrode for 3 cells in LIBs.
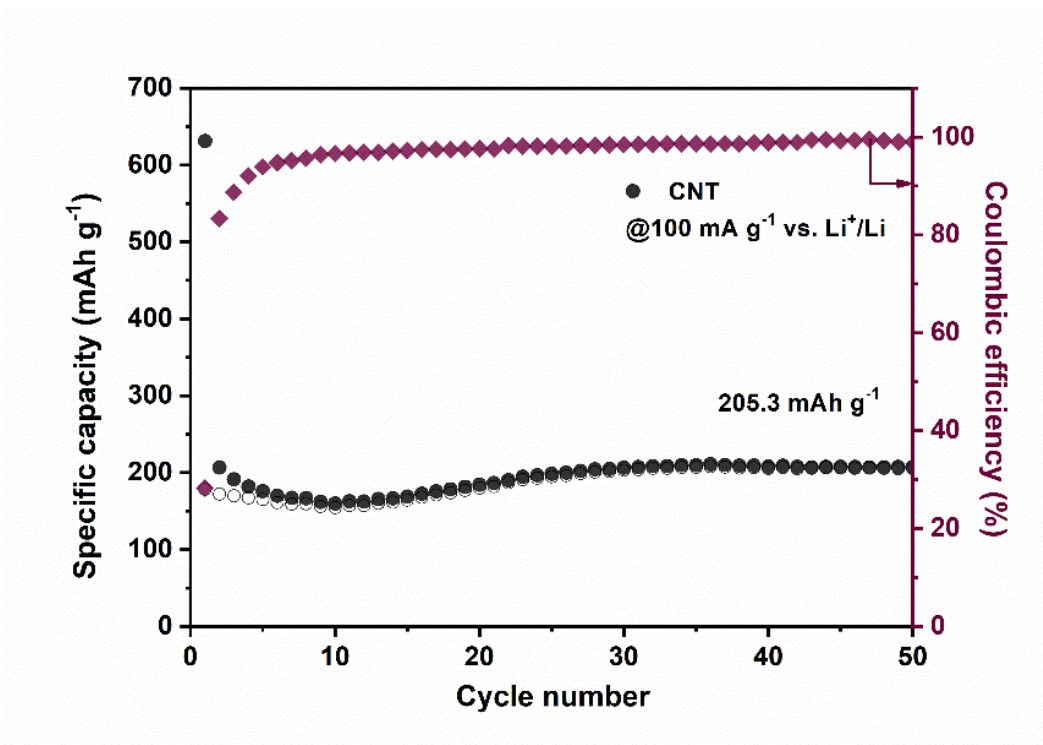
Fig. S12. Cycling performance of CNTs for LIBs. Specific capacity of CNTs at 100 mA g^{-1} vs. Li$^+$/Li.

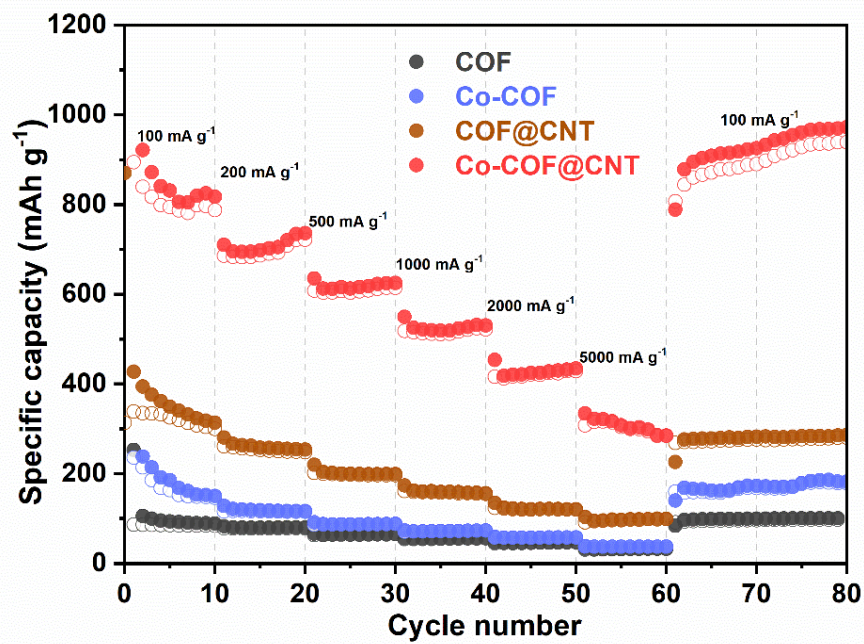**Fig. S13. Rate capabilities of TP-BPY-COF, Co-COF, COF@CNT, and Co-COF@CNT electrodes for LIBs.**
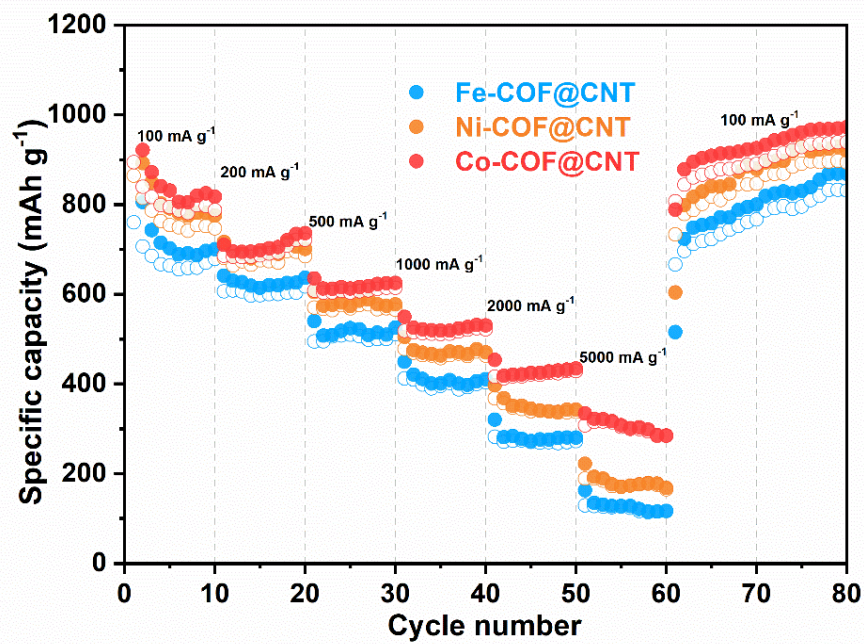
Fig. S14. Rate capabilities of Fe-COF@CNT, Ni-COF@CNT, and Co-COF@CNT for LIBs.
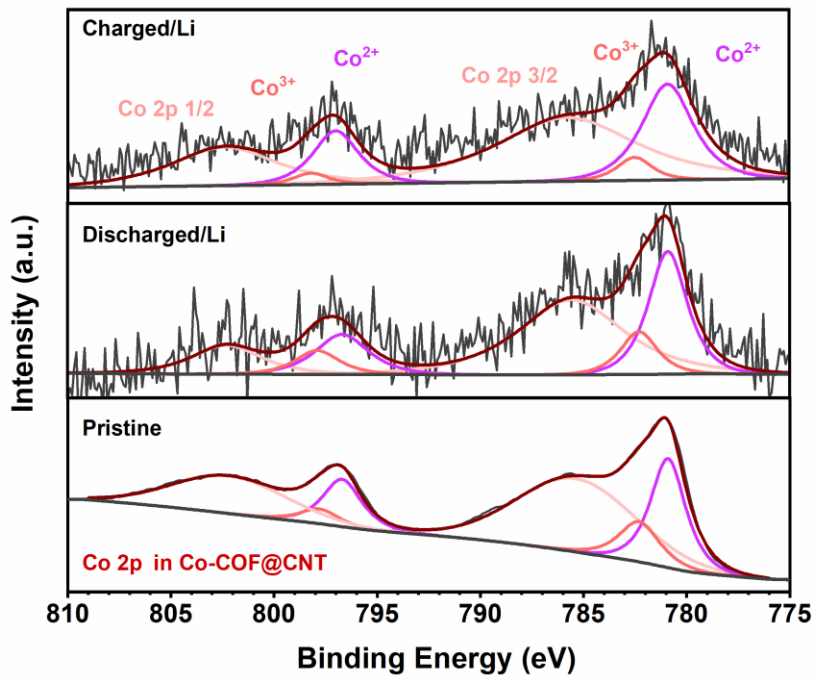
Fig. S15. XPS results of the Co 2p spectrum during the lithiation and delithiation process.
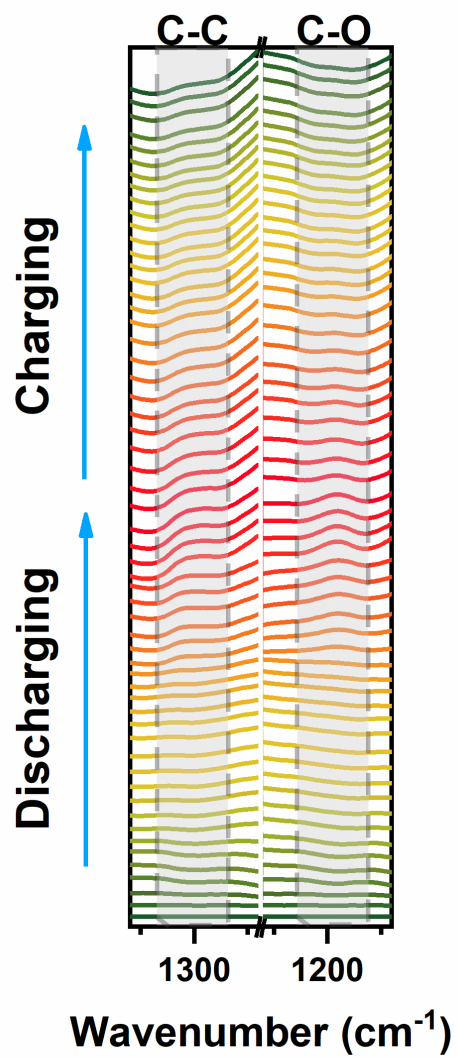
Fig. S16. *In-situ* **FT-IR spectra of the Co-COF@CNT electrode in LIBs. Notes:** upward indicates the generation.
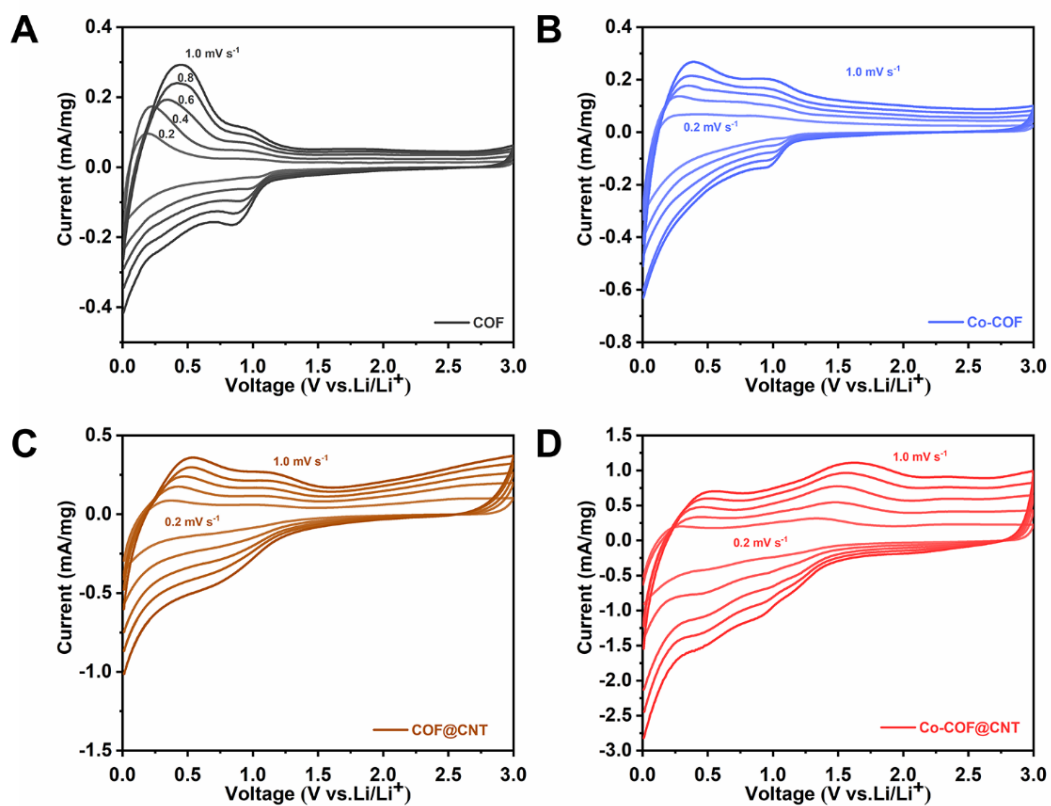
Fig. S17. CV curves at different scan rates ranging from 0.2 to 1.0 mV s^{-1} vs. Li$^+$/Li. (**A**) TP-BPY-COF, (**B**) Co-COF, (**C**) COF@CNT, and (**D**) Co-COF@CNT.
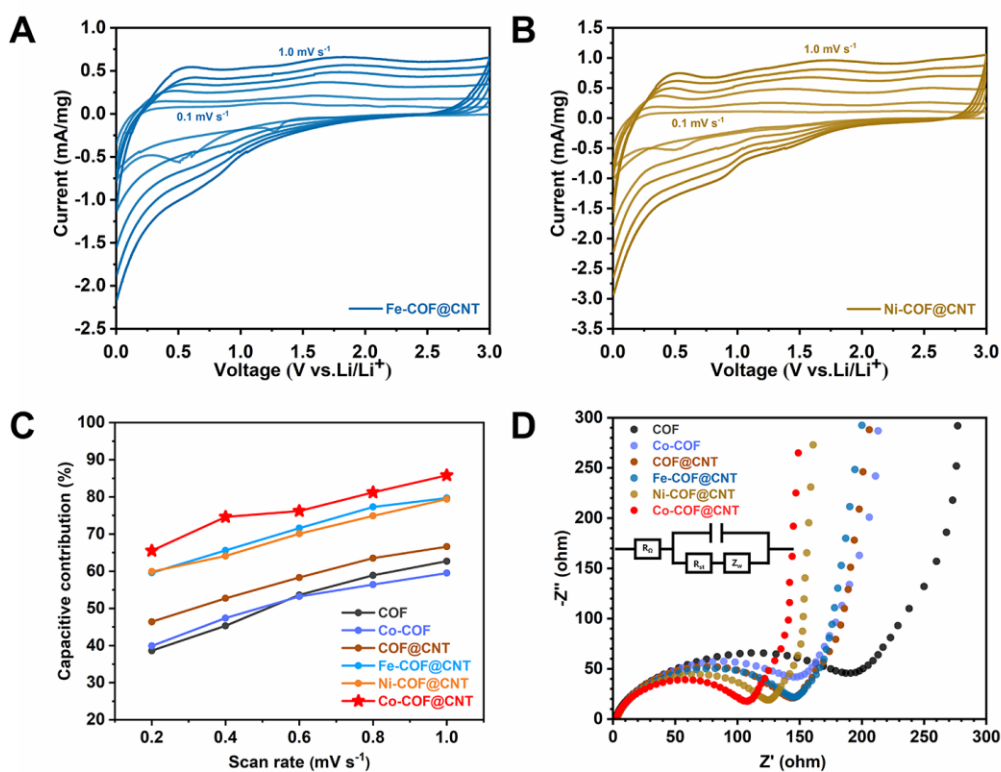
Fig. S18. CV curves at different scan rates ranging from 0.1 to 1.0 mV s⁻¹ vs. Li⁺/Li. (**A**) Fe-COF@CNT, and (**B**) Ni-COF@CNT. (**C**) The capacitive contribution and (**D**) Nyquist plots of TP-BPY-COF (black), Co-COF (purple), COF@CNT (brown), Fe-COF@CNT (blue), Ni-COF@CNT (yellow), and Co-COF@CNT (red) vs. Li⁺/Li.
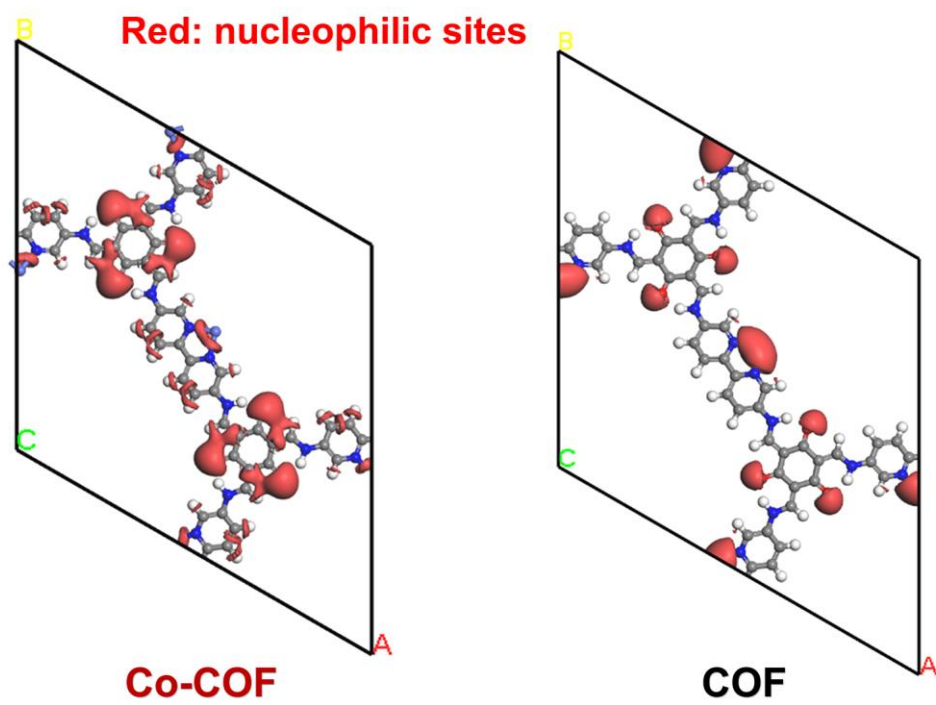
Fig. S19. The spatial distribution calculated by the Fukui function for Co-COF and COF to exhibit the nucleophilic sites.
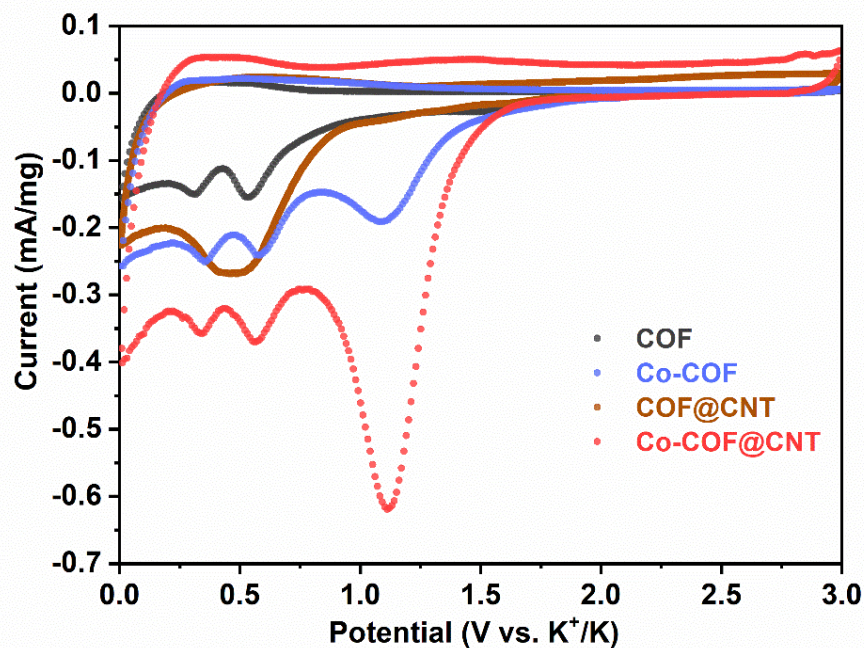
Fig. S20. CV curves of the TP-BPY-COF, Co-COF, COF@CNT, and Co-COF@CNT electrodes for PIBs during 0.01-3.0 V at 0.1 mV s⁻¹. Notes: TP-BPY-COF (black), Co-COF (purple), COF@CNT (brown), and Co-COF@CNT (red).
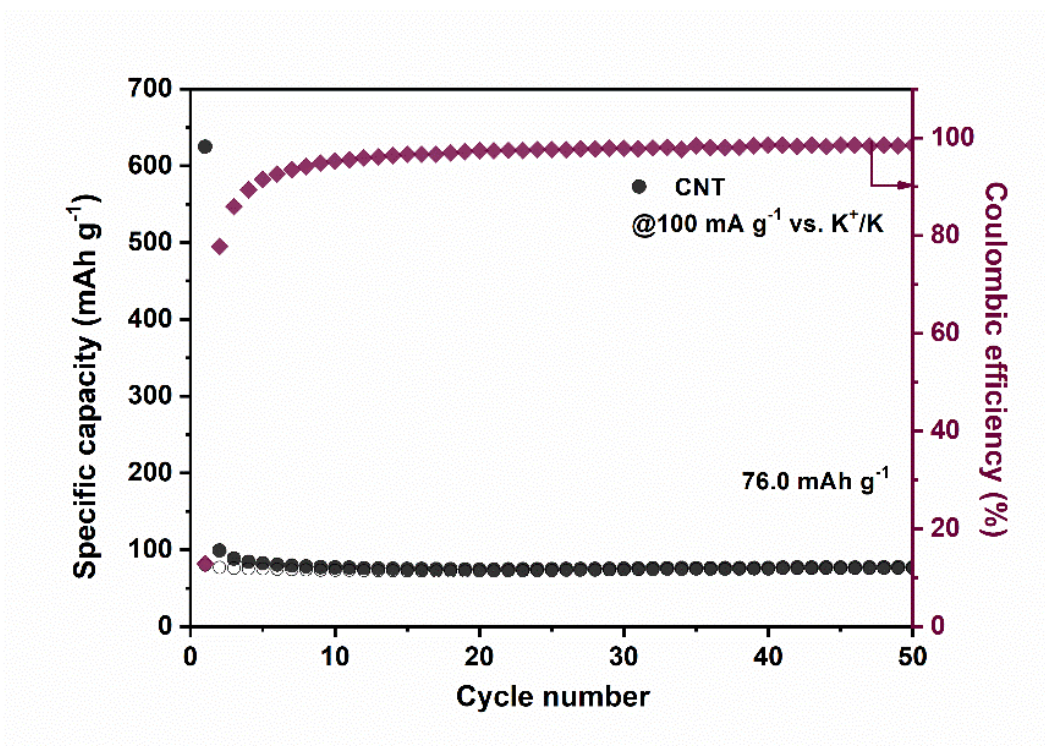
Fig. S21. Cycling performance of CNTs for PIBs. Specific capacity of CNTs at a high current density of 100 mA g^{-1} vs. K$^+$/K.
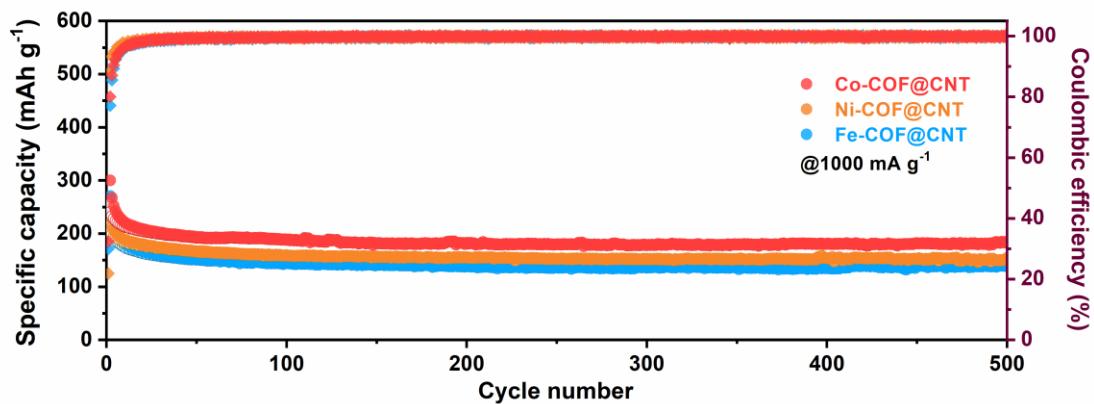
Fig. S22. Cycling performances of Fe-COF@CNT, Ni-COF@CNT, and Co-COF@CNT for PIBs. Specific capacity of Fe-COF@CNT, Ni-COF@CNT, and Co-COF@CNT at a current density of 1000 mA g^{-1} vs. K^+/K.

Fig. S23. XPS results of the Co 2p spectrum during potassiation and de-potassiation process.
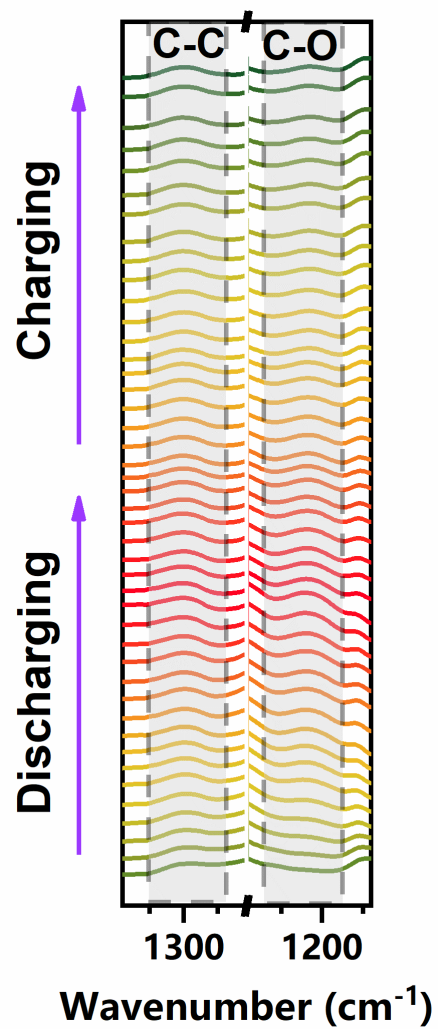
Fig. S24. *In-situ* **FT-IR spectra of the Co-COF@CNT electrode in PIBs. Notes:** upward indicates the generation.
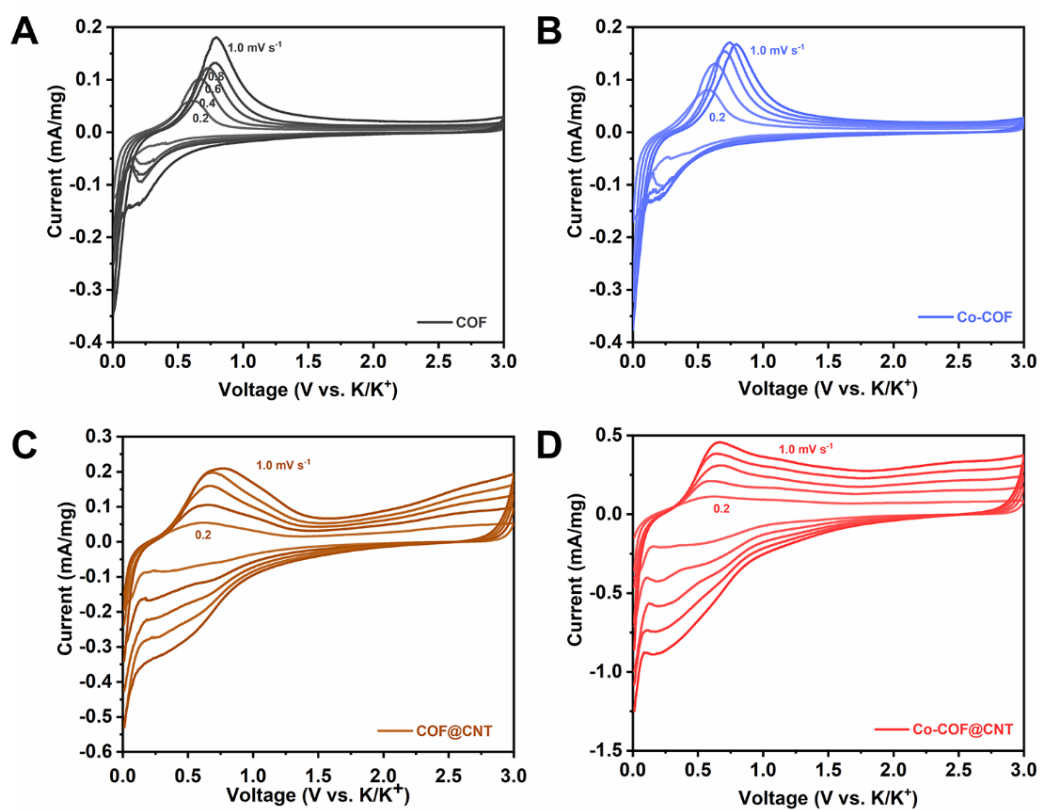
Fig. S25. CV curves at different scan rates ranging from 0.2 to 1.0 mV s⁻¹ vs. K⁺/K. (**A**) TP-BPY-COF, (**B**) Co-COF, (**C**) COF@CNT, and (**D**) Co-COF@CNT.
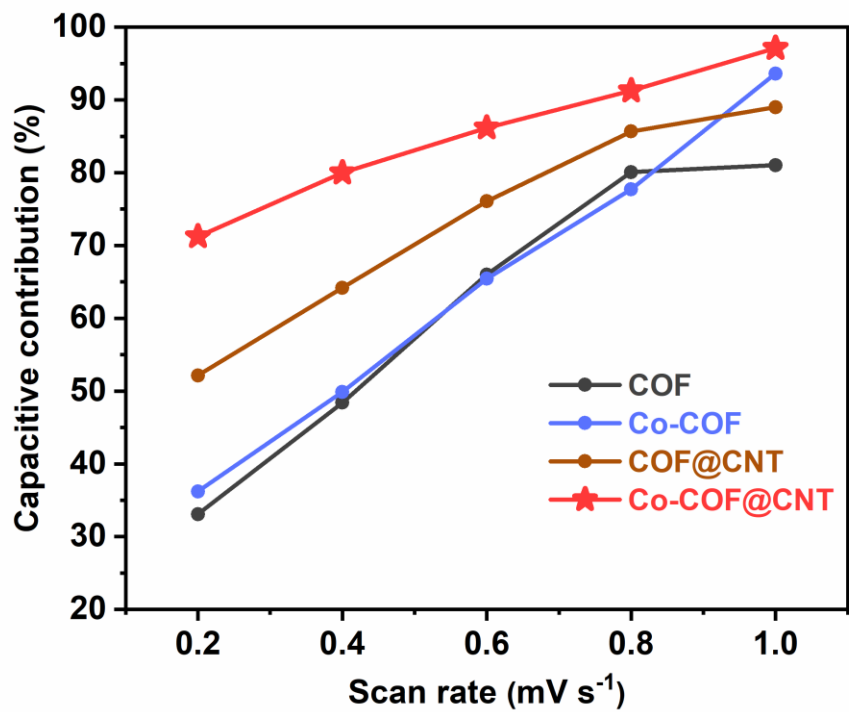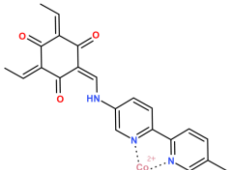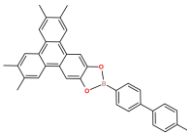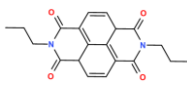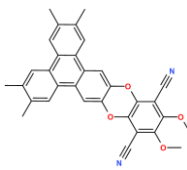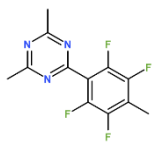
Fig. S26. The capacitive contribution of TP-BPY-COF (black), Co-COF (purple), COF@CNT (brown), and Co-COF@CNT (red) in PIBs.

Table S1. K-edge fitting parameters of Co-COF.

| Sample	shell	N	R [Å]	ΔE_0 [eV]	σ^2 [10^{-3}Å^2]	R-factor
Co-COF	Co-N	2	2.14	2.75	3.0	1.7%
Co-COF	Co-O	4	2.00	−7.60	7.5	1.7%

N: coordination numbers; R: the internal atomic distance; σ^2: Debye-Waller factor; ΔE_0: the edge-energy shift.

Table S2. Electrochemical properties comparison between Co-COF@CNT and previous related organic polymer anodes for PIBs.

Materials	Retained Reversible Capacity [mA h g^{-1}]	Cycle Number/ Current Density [mA g^{-1}]	Rate Capacity @Current Density [mA g^{-1}]	Ref.
Co-COF@CNT **449**	**150/100**	**301@500**	**This work**
185	**500/1000**	**184@2000**	
COF-10@CNT 288	500/100	~200@500 ~100@2000	*ACS Nano* **2019**, *13*, 3600
PIM@KB 110	500/100	130@500 118@2000	*Small* **2020**, *16*, 2002953
COF@Co 371	400/100	~160@500 105@2000	*ACS Appl. Mater. Interfaces* **2021**, *13*, 48913-48922
E-FCTF 228	100/100	~150@500 58@2000	*ACS Nano* **2019**, *13*, 14252
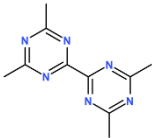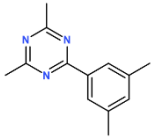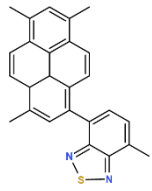
CTF-0	113	200/100	~84@500 63@1000	*Chem. Sci.* **2019**, *10*, 7695
CTF-1	60	200/100	~39@500 31@1000	*Chem. Sci.* **2019**, *10*, 7695
PyBT	272	500/50	~200@200 104@500	*ACS Nano* **2019**, *13*, 745

Table S3. Electrochemical properties comparison between Co-COF@CNT and previous representative carbon anodes for PIBs.

Materials	Retained Reversible Capacity [mA h g^{-1}]	Cycle Number	Current Density [mA g^{-1}]	Ref.
Co-COF@CNT	**449**	**150**	**100**	**This work**
	185	**500**	**1000**	
CNC (carbon nanocage)	195	100	200	*Adv. Energy Mater.* **2018**, *8*, 1801149
GNC-600 (N-doped)	280	/	50	*Adv. Funct. Mater.* **2019**, *29*, 1903641
NCNF-650 (N, O-doped)	248	25	100	*Nat. Commun.* **2018**, *9*, 1720
CNFF (carbon nanofiber)	158	2000	1000	*Nano Lett.* **2018**, *18*, 7407
PNCM (N-doped)	260	120	100	*Adv. Mater.* **2017**, *29*, 1702268
Hollow carbon (N-doped)	340	/	100	*J. Am. Chem. Soc.* **2018**, *140*, 7127
NHC (N-doped)	161	1600	1000	*Energy Environ. Sci.* **2019**, *12*, 1605
N-HPC (N-doped)	292	400	100	*Nano Lett.* **2019**, *19*, 4965
NPC (N-doped)	342	500	100	*Adv. Energy Mater.* **2018**, *8*, 1802386
FFGF (F-doping)	165	200	500	*ACS Appl. Mater. Interfaces* **2016**, *8*, 20682
S-RGO-600 (S-doping)	297	/	100	*Nano Energy* **2018**, *53*, 415
SNHC (S, N-doped)	213	500	100	*Adv. Energy Mater.* **2019**, *9*, 1901379
NOHPHC (N, O-doped)	130	1100	1050	*Adv. Mater.* **2018**, *30*, 1700104

PCMs (S, O-doped)	108	2000	1000	*Adv. Energy Mater.* **2018**, *8,* 1800171
PHC-700 (P, O-doped)	260	1000	200	*Adv. Energy Mater.* **2019**, *9,* 1901676
N, P-VG@CC (N, P-doped)	345	1000	25	*Small* **2019**, *15,* 1901285